

Percolation through Voids around Overlapping Spheres, a Dynamically based Finite Size Scaling Analysis

D. J. Priour, Jr¹

¹*Department of Science, Kansas City Kansas Community College, Kansas City, KS 66112, USA*
(Dated: November 13, 2018)

The percolation threshold for flow or conduction through voids surrounding randomly placed spheres is rigorously calculated. With large scale Monte Carlo simulations, we give a rigorous continuum treatment to the geometry of the impenetrable spheres and the spaces between them. To properly exploit finite size scaling, we examine multiple systems of differing sizes, with suitable averaging over disorder, and extrapolate to the thermodynamic limit. An order parameter based on the statistical sampling of stochastically driven dynamical excursions and amenable to finite size scaling analysis is defined, calculated for various system sizes, and used to determine the critical volume fraction $\phi_c = 0.0317 \pm 0.0004$ and the correlation length exponent $\nu = 0.92 \pm 0.05$.

PACS numbers: 64.60.ah,61.43.-j,64.60.F-,61.43.Gt

I. INTRODUCTION

Notwithstanding simple underlying Physics, percolation transition are *bona fide* second order phase transitions, with all of usual the hallmarks of singular behavior at a critical point¹. Percolation transitions, phase transitions mediated by a disordering influence such as the random removal of sites or bonds on a regular lattice geometry, are amenable to numerical study in the context of Monte Carlo calculations used to treat disorder. However, while the critical behavior in discrete systems may be characterized to a high level of precision in this manner, there are salient examples of percolation phenomena which cannot be reduced to discrete lattices.

In realistic porous media, the flow of liquid on a macroscopic basis typically entails the passage of liquid around irregularly shaped granules which comprise the material and represent barriers to fluid flow. For the movement of fluid or charge in porous materials, there is a dichotomy for volume concentrations of barrier particles above and below a critical concentration ρ_c . If inclusions are sufficiently sparse, voids join together in a macroscopic connected network spanning the entire system, allowing for the transmission of fluid at the bulk level. On the other hand, for large enough concentrations of randomly placed barrier particles, contiguous navigable voids are limited in size to a finite length scale ξ , barring the transmission of fluid at a system wide level; the critical density ρ_c of inclusions which separates the two scenarios is thus of practical significance.

For the sake of convenience, we rescale coordinates in such a way that the spherical inclusions are each of unit radius. Although in principle one may record the critical density ρ_c where the percolation transition occurs, a more frequent practice in discussing percolation through voids is to report instead the excluded volume², given by $\phi_c = e^{-\frac{4\pi}{3}\rho_c}$.

Determining if voids may be traversed at the macroscopic level is a continuum percolation problem for which a topologically equivalent discrete counterpart is in gen-

eral not readily accessible, a condition very distinct from that of a complementary percolation problem (with the permeability pattern reversed) where the flux occurs through networks formed of overlapping included particles with interstitial regions impervious to fluid flow. The geometry of the randomly placed barriers, known *a priori*, facilitates the calculation of characteristics related to percolation when the flow is through included particles instead of the interstitial spaces. On the other hand, the fact that the shapes of voids between barrier particles are only evident *a posteriori* hampers a rigorous identification of networks formed by connected voids and enhances the challenge of finding the percolation threshold. Nevertheless, with the aid of a finite size scaling analysis, we determine not only the critical volume fraction ϕ_c , but also the critical exponent ν associated with the correlation length ξ .

Previous theoretical studies include calculations which use an approximate discrete scheme and extrapolate to the continuum case^{3,4}. In a related effort, the discretization scheme has been applied to randomly placed ellipsoids⁵ and oblate spheroids⁶. In particular cases, such as systems comprised of randomly placed spheres, discrete networks equivalent to void spaces⁷ may be constructed. Voronoi tessellations, and the appropriate generalizations have been applied⁸⁻¹⁰ to systems comprised of randomly located spheres. In a recent set of calculations, there is no discretization scheme and the simulation entails following tracer particles in an effectively infinite sized system^{11,12}; the percolation threshold is identified by determining the density of spheres for which the tracers cease to move diffusively. In this work, we use a dynamical approach where systems of finite size are examined. In this way, we are able to apply standard machinery of finite size scaling analysis while providing rigorous treatment to the geometric intricacies of voids between barriers which serve as conduits for fluid or charge in the percolative regime.

II. CALCULATION OF THE EXCURSION ORDER PARAMETER

An order parameter, an intensive thermodynamic variable finite when the phase is intact, and decreasing continuously to zero at a phase boundary (e.g. magnetization per unit volume in the case of ferromagnetism disrupted by thermal fluctuations above the Curie Temperature and nonzero below it), may be pressed into service as a tool to locate second order phase transitions and thereby determine the phase diagram. In percolation phenomena where connected navigable clusters are readily identified, the “strength” of the spanning cluster, or the number of sites in the lattice it encompasses relative to the total number of sites in the system, is conveniently sampled in Monte Carlo simulations using techniques such as the Hoshen-Kopelman algorithm for the identification and characterization of connected clusters¹³.

In the scenario of interest, where percolation occurs through irregularly shaped interstices among randomly placed barrier particles of a prescribed shape, the connectivity of void volumes to adjacent navigable regions may be difficult to establish in more general situations (e.g. non-spherical inclusions such as tetrahedra, cubes, or octahedra). To address this challenge, we use dynamical simulations to probe and determine the extent of voids. Although stochastically driven exploration is validated in the case of randomly placed spheres, the approach may be used in scenarios where variants of Voronoi tessellation are more difficult to apply.

In the spirit of a *Gedanken* experiment, we envision applying a reflective coating to exposed surfaces of overlapping spheres such that light striking the included particles is reflected with no penetration of the incident rays. Whereas the transmission of light through the matrix of inclusions would signal that the system would admit the flow of fluid or electrical charge, a configuration which blocks the transmission of incident light also lacks a percolating path.

Dynamical trajectories are initiated with an unbiased choice for the point of origin in the interior of a void and exterior to all barrier particles. To select a void point, randomly chosen candidate locations are accepted only if the point is exterior to all neighboring spheres. Some economy is gained in partitioning the 3D system into a cubic grid, where the unit cell size is slightly greater than the radius r of the spheres. The subdivisions reduce the task of checking for penetration into nearby spheres to simply checking the cubic unit cell occupied by the prospective (randomly chosen) starting point as well as each of the adjacent cubes. To set the virtual ray in motion, a “velocity” vector \hat{v} is randomly chosen in a spherically symmetric way to eliminate any directional bias, with \hat{v} of unit length since “speed” has no physical or computational significance in the context of the order parameter calculation.

The ray trajectory is $\vec{x}_l = \vec{x}_0 + \hat{v}t$ with the start-

ing point \vec{x}_0 and the orientation of the velocity vector \hat{v} stochastically determined. The path of the ray must be traced until contact is made with the nearest sphere; with a barrier particle centered at \vec{x}_c , the condition for intersection with a sphere of radius r is $|\vec{x}_l - \vec{x}_c| = r$. Standard geometric arguments lead to $d_{\text{coll}} = -x_d \cos \theta \pm \sqrt{1 - x_d^2 \sin^2 \theta}$ for the distance to a point of intersection, where $x_d \equiv |\vec{x}_0 - \vec{x}_c|$ and $\cos \theta \equiv \frac{\vec{x}_d \cdot \vec{x}_d}{|\vec{x}_d|}$. Choosing the negative sign corresponds to the closer point of entry and the positive sign to the more distant point of departure as the ray propagates through and exits from the sphere. Finding the closest included particle intersected by the ray is tantamount to minimizing d_{coll} , the shortest distance to a sphere along the trajectory.

To reduce computational overhead, the system is subdivided into a cubic grid in the same fashion as used to determine if a randomly chosen point is located in a void; rays are propagated from one small unit cell to the next until a collision with a barrier particle is recorded. At the site of a collision \vec{x}_{coll} , to avoid penetration of the impermeable particles comprising the matrix, the direction of motion must change in such a way that the incident ray is projected away from the interior of the barrier particle. Specular reflection is implemented by reversing the component of the velocity in the direction of $\vec{x}_{\text{coll}} - \vec{x}_c$, the radius vector extending from the sphere center to the site of the collision.

Although mirror reflection encapsulates the physics of geometric optics appropriate to a ray of light moving in a matrix of silvered spheres, propagation by simple specular reflection may be improved on, particularly in the case of neck-like voids where many collisions may be required to traverse the narrow corridor if the ray is directed normal to the primary axis of the void. To improve the efficiency of navigation by roughly an order of magnitude, we incorporate moves where, instead of mirror reflection, the ray trajectory shifts by a right angle. In 3D, even with a perpendicular shift imposed, there remains a degree of freedom, which is selected at random to provide stochastic input at each collision. The balance of the moves is such that stochastically infused right angle moves outnumber specular moves two to one.

To interrogate the system and determine whether a void is part of a spanning cluster, we calculate the excursion parameter $\tilde{\delta} = \frac{1}{3L}(\delta_{\text{rms}}^x + \delta_{\text{rms}}^y + \delta_{\text{rms}}^z)$, structured to allow for the incorporation of statistical information gleaned from traversals along each of the three Cartesian axes. In calculating the rms deviations, special consideration must be given the periodicity of the system. When the density of randomly placed spheres is high enough to block percolation, where $\phi < \phi_c$, the scale ξ of contiguous void networks is in most cases small relative to the system size, and accordingly, $\tilde{\delta} \ll 1$.

On the other hand, if inclusions are sparse enough that $\phi > \phi_c$, system wide traversal becomes feasible. Moreover, with periodic boundary conditions imposed

the RMS deviations along one or more axes could in principle grow without bound as the ray propagates from one replica of the system to the next. In such situations, the result would be an unrealistically large order parameter, a circumstance which may be remedied by truncating δ_{rms}^x and counterparts along other axes at the system size L . Thus, in the extreme case of a system devoid of inclusions, $\tilde{\delta}$ would attain its maximum value of 1. The excursion quantity $\tilde{\delta}$, which saturates at unity in the absence of obstacles and falls to zero at the percolation threshold for bulk systems, serves as an order parameter giving a measure of the size of a randomly selected void. In the thermodynamic limit, the configuration averaged $\tilde{\delta}$ also gives the probability that a randomly selected void is a system spanning cavity.

In a diffusive excursion, though the disorder and time averaged vector displacement vanishes, the root mean square distance traveled scales as $N_{\text{coll}}^{1/2}$, where N_{coll} is the number of ray interactions (and concomitant trajectory deflections) with barrier particles. Unless one is precisely at the percolation threshold with RMS deviations from the trajectory starting point scaling as N_{coll}^ϵ , where $\epsilon < 1/2$ in the non-diffusive critical regime^{11,12}, configuration averaged ray excursions will scale diffusively with the number of sphere interactions, if the system is sufficiently large.

If the void is small in size, a ray which propagates in the cavity will probe its extent relatively quickly, yielding a finite $\tilde{\delta}$ value. On the other hand, with a system spanning void scaling as the system size L , the ray traversal time varies as L^2 on average. Hence, to avoid a spuriously low result for the percolation threshold ϕ_c , trajectories are propagated with collisions accumulating until $N_{\text{coll}} \gg \eta L^2$ where η is an integer prefactor. By successively doubling η , a saturation point is eventually found (i.e. for $\eta = 80,000$ and $\eta = 160,000$) where statistically significant changes in critical quantities cease to occur.

The calculation of the $\tilde{\delta}$ parameter entails averaging over many realizations of disorder (i.e. at least 10^4) to suppress statistical fluctuations and permit the observation of finite size scaling trends, which are exploited to calculate critical quantities such as ϕ_c and the correlation length exponent ν . To generate disorder configurations, we sample the grand canonical ensemble as described in the Appendix to determine the number of spherical barriers encompassed in the simulation volume. The Mersenne Twister algorithm, which generates high quality random numbers with a modest computational cost, is used for stochastic input.

III. FINITE SIZE SCALING ANALYSIS

Percolation transitions, whether in the context of continuum or in discrete cases, are second order transitions with singular behavior in thermodynamic variables at the phase transition. Single parameter finite size scaling analysis posits a form $L^\alpha f([\phi - \phi_c]L^{1/\nu})$ for ther-

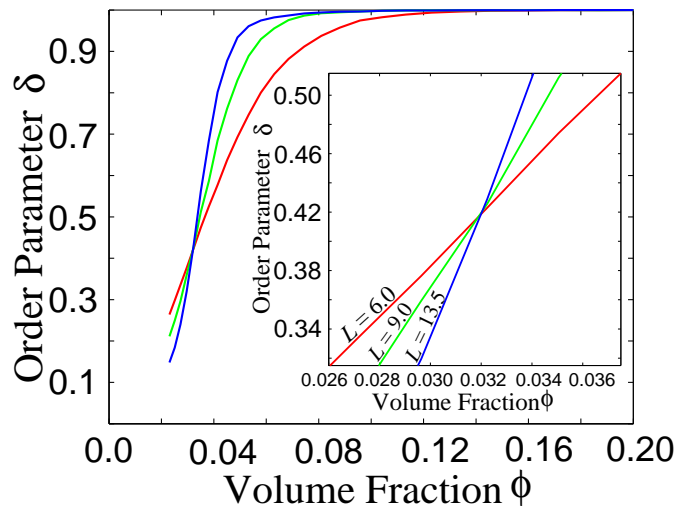


FIG. 1: (Color online) The excursion order parameter $\tilde{\delta}$ is plotted with respect to excluded volume ϕ for various system sizes; the inset is a magnified view of the intersection of the $\tilde{\delta}$ curves.

modynamic variables, a singular form anticipated for the excursion order parameter $\tilde{\delta}$. Since $\tilde{\delta}$ is normalized and thus dimensionless, $\alpha = 0$, and the singular dependence reduces to $\tilde{\delta} \sim f([\phi - \phi_c]L^{1/\nu})$. An important implication is the crossing of $\tilde{\delta}$ curves at ϕ_c for different system sizes, provided the system size is large enough. Similar intersections are seen in the case of the Binder cumulant¹⁶ at the Curie temperature T_c in the context of ferromagnetic transitions, and the crossing phenomena in both the former and the latter represent a robust avenue for locating second order phase transitions.

Fig. 1 shows $\tilde{\delta}$ curves for different system sizes (i.e. $L = 6.0$, $L = 9.0$, and $L = 13.5$) with a well defined crossing at a common point. To determine ϕ_c in a systematic fashion, we calculate the order parameter for pairs of system sizes (e.g. $\{6, 9\}$ and $\{8, 12\}$) with the larger member of each pair 1.5 times the size of the smaller. Although in the thermodynamic limit crossings would occur exactly at ϕ_c , the locations of intersections for finite size systems [e.g. $\phi_c(\bar{L})$] differ slightly from ϕ_c due to finite size effects, and must be considered pseudocritical points¹⁴. The pseudo-critical excluded volume $\phi_c(\bar{L})$ for each pair are recorded in table I and also appear in the graph in Fig. 2, with the system size reciprocal \bar{L}^{-1} on the abscissa. For small system sizes, $\phi_c(\bar{L})$ rises, eventually saturating at 0.0317 ± 0.0004 , the extrapolated result for the percolation threshold.

A complementary finite size scaling technique for calculating the percolation threshold ϕ_c , based on the data collapse phenomenon in the critical region, simultaneously takes into consideration results for a broad range of system sizes and also yields the correlation length exponent ν .

Data collapse graphs may be prepared by plotting on the vertical axis the quantity $\tilde{\delta}$ with $L^{1/\nu}|\phi - \phi_c|$ (with

L_1	L_2	\bar{L}	$\phi_c(\bar{L})$
5.0	7.5	12.25	0.03015(24)
6.0	9.0	7.5	0.03118(17)
7.0	10.5	8.75	0.03177(15)
8.0	12.0	10.0	0.03214(12)
9.0	13.5	11.25	0.03209(14)
10.0	15.0	12.5	0.03190(17)
12.0	18.0	15.0	0.03230(20)
13.5	20.25	16.875	0.03166(13)
14.0	21.0	17.5	0.03180(14)
16.0	24.0	20.0	0.03165(13)

TABLE I: $\tilde{\delta}$ curve intersection results with for various \bar{L} values

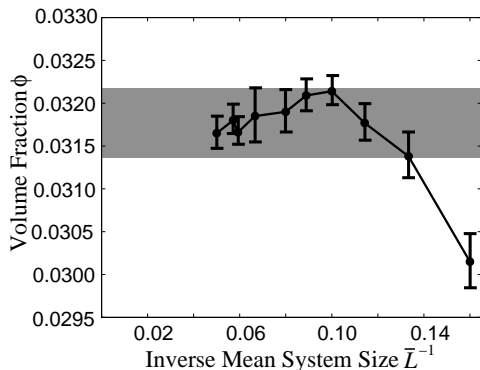


FIG. 2: (Color online) Pseudocritical excluded volumes (with calculated error bars) plotted with respect to the reciprocal of the mean system size \bar{L} for each pair

an optimal collapse for quantitatively correct values for ν and ϕ_c) on the abscissa for various systems sizes. The coincidence of data on the same curve is a manifestation of the existence of a universal singular scaling function for $\tilde{\delta}$ as well as an indication that ν and ϕ_c are specified correctly.

To use the data collapse as a quantitative tool, one notes that the “v” shaped curve in Fig. 3 is essentially

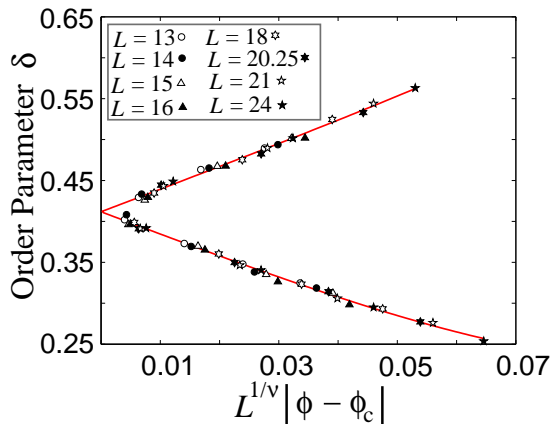


FIG. 3: (Color online) Data collapse with $\tilde{\delta}$ data shown for various system sizes. The solid red line is a polynomial curve determined from a nonlinear least squares fit, and symbols represent data from Monte Carlo simulations.

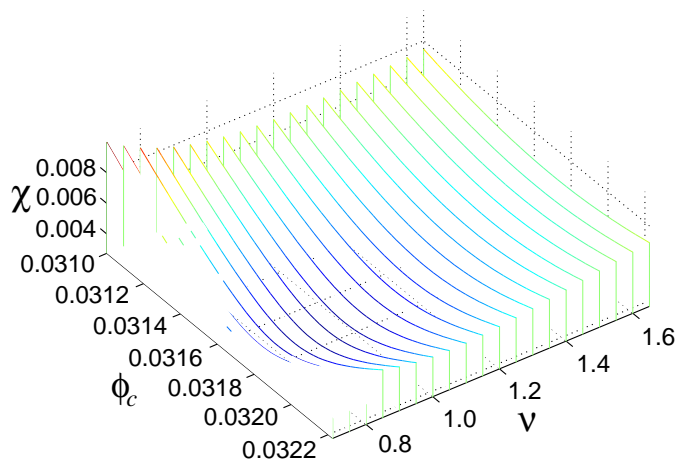


FIG. 4: (Color online) χ plot shown with respect to the correlation length critical exponent ν and the excluded volume ϕ_c with global minimum at $\nu = 0.92$ and $\phi_c = 0.0317$.

linear with a small degree of curvature. To accommodate this quasi-linear variation in a perturbative fashion, we use a form $f(x) = A_0 + A_1x + \dots + A_4x^4$ (the results are not impacted by the inclusion of the quartic term, and the series is truncated at fourth order) with $x \equiv L^{1/\nu}(\phi - \phi_c)$. To assess the degree to which the points from Monte Carlo calculations lie on the same curve, we use

$$\chi(\phi_c, \nu, A_0, \dots, A_4) = \sqrt{\sum_i \left[\frac{f(x_i) - \tilde{\delta}_i}{\tilde{\delta}_i} \right]^2}. \quad (1)$$

The quantity χ provides an overall measure of the deviation of Monte Carlo data from the scaling curve. Hence, optimizing the data collapse entails minimizing χ with respect to ϕ_c , ν , and the A_i parameters with a two tiered fit. First, for a particular choice of ν and ϕ_c , the parameters A_i are calculated in a linear least squares fit. The appropriate values of the critical indices ϕ_c and ν are then determined by a stochastically driven least squares fit, where a sequence of attempts are made to introduce small random perturbations to ϕ_c and ν , with the shifts accepted only if the sum of squares term χ is thereby lowered. Fig. 4 shows χ with respect to ν and ϕ_c . The global minimum for $\phi = 0.0317$ and $\nu = 0.92$ is, within the bounds of Monte Carlo statistical error, consistent with the calculation of ϕ_c based on crossings of the $\tilde{\delta}$ quantity. Moreover, the calculated value of ν is in accord with results gleaned from high precision Monte Carlo calculations for discrete 3D systems (e.g. 0.875[1] for discrete percolation models on 3D lattices with cubic symmetry¹⁵).

IV. CONCLUSIONS

We have used a large-scale Monte Carlo calculation based on a dynamical exploration of void spaces to determine the critical properties (i.e. finding $\phi_c = 0.0317 \pm$

0.0004 and $\nu = 0.92 \pm 0.05$) for the percolation through voids surrounding randomly placed impermeable spheres. Two complementary finite size scaling analyses yield the same percolation threshold ϕ_c . Our dynamically based calculation is distinct in that it makes no approximation for the structure of void spaces, while also incorporating finite size effects which are exploited to calculate critical indices. The result for the correlation length critical exponent ν is compatible with the critical behavior of discrete 3D counterparts.

V. APPENDIX: SAMPLING THE POISSONIAN DISTRIBUTION

To sample realizations of disorder from the appropriate statistical distribution, it is important to generate random configurations of spherical inclusions in an unbiased way; since we operate in the grand canonical ensemble, the number N of spheres in the simulation volume must in general vary from one sample to the next due to statistical fluctuations. The integer value closest to the mean occupancy $N_{\text{av}} = \rho L^3$ is a convenient initial choice, and random variations in the number of spheres in the system are taken into consideration with a sequence of stochastically driven attempts either to raise or lower N . The latter are part of an importance sampling scheme similar to that used to derive the Metropolis criterion¹⁷ at the heart of Monte Carlo simulations that sample the Boltzmann distribution in the calculation of equilibrium thermodynamic variables.

To determine the probability of having N spheres in the simulation volume $v = L^3$, we divide v into M subvolumes of equal size where $\Delta v = v/M$. For large M the likelihood of multiple occupancy in any of the subvolumes

is very small relative to the chance of having one or zero sites in a subdivision; in the small Δv limit, the single occupancy probability is $\rho\Delta v$, with $(1 - \rho\Delta v)$ being the complementary likelihood of null occupancy. Hence, the probability that the entire system is devoid of hopping sites is $(1 - \rho v/M)^M$, which becomes $e^{-\rho v}$ for $M \rightarrow \infty$. For single occupancy, adopting a prefactor M to take into consideration that the site may reside in any of the M subvolumes, yields $M(\rho v/M)(1 - \rho v/M)^{M-1}$, which becomes $\rho v e^{-\rho v}$ in the $\Delta v \rightarrow 0$ limit. Similar logic gives $P(N) = e^{-\rho v}(\rho v)^N/N!$ for the general case of exactly N spheres in the simulation volume, where $N!$ compensates for multiple occupancy.

To generate a disorder realization, a succession of attempts (a number of moves in the vicinity of N_{av} is sufficient to achieve ergodicity) is made to raise or lower the occupancy number N , where the choice to increase or decrease N is randomly determined. For increments from N to $N + 1$, the change is accepted if $X_r < r_+ \equiv p(N + 1)/p(N) = \rho v/(N + 1)$, where X_r is a random number sampled uniformly from the interval $[0,1]$. Similarly, decreasing N to $N - 1$ occurs if $X_r < r_- \equiv p(N - 1)/p(N) = N/\rho v$. Finally with N properly sampled, three Cartesian coordinates for each sphere are chosen independently (and at random with uniform probability density) from the interval $[0, L]$.

Acknowledgments

Numerical calculations have benefited from the University of Maryland 280 node High Performance Computing Cluster (HPCC) as well as the University of Missouri Lewis Cluster.

-
- ¹ D. Stauffer and A. Aharony, *Introduction to Percolation Theory*, 2nd ed. (Taylor and Francis, Bristol, 1992).
- ² R. Zallen, *The Physics of Amorphous Solids* (Wiley-VCH, Weinheim, 1983).
- ³ N. S. Martys, S. Torquato, and D. P. Bentz, *Phys. Rev. E* **50**, 403 (1994).
- ⁴ R. S. Maier, D. N. Kroll, H. T. Davis, and R. S. Bernard, *J. Colloid Interface Sci.* **217**, 341 (1999).
- ⁵ Y. B. Yi, *Phys. Rev. E* **74**, 031112 (2006).
- ⁶ Y. B. Yi and K. Esmail, *J. Appl. Phys.*, **111**, 124903 (2012).
- ⁷ A. R. Kerstein, *J. Phys. A* **16**, 3071 (1983).
- ⁸ W. T. Elam, A. R. Kerstein, and J. J. Rehr, *Phys. Rev. Lett* **52**, 1516 (1984).
- ⁹ S. C. van der Marck, *Phys. Rev. Lett.* **77**, 1785 (1996).
- ¹⁰ M. D. Rintoul, *Phys. Rev. E* **62**, 68 (2000).
- ¹¹ F. Höfling, T. Munk, E. Frey, and T. Franosch, *J. Chem. Phys.* **128**, 164517 (2008).
- ¹² M. Spanner, F. Höfling, G. E. Schröder-Turk, K. Mecke, and T. Franosch, *J. Phys.: Condens. Matter* **23**, 234120 (2009).
- ¹³ J. Hoshen and R. Kopelman, *Phys. Rev. B* **14**, 3438 (1976).
- ¹⁴ K. Chen, A. M. Ferrenberg, and D. P. Landau, *Phys. Rev. B* **48**, 3249 (1993).
- ¹⁵ C. D. Lorenz and R. M. Ziff, *Phys. Rev. E* **57**, 230 (1998).
- ¹⁶ D. P. Landau and K. Binder, *A Guide to Monte Carlo Simulations in Statistical Physics*, (Cambridge, 2000).
- ¹⁷ N. Metropolis, A. W. Rosenbluth, M. N. Rosenbluth, A. H. Teller, E. Teller, *J. Chem. Phys.* **21**, 1087 (1953).